A retrospective evaluation of Bayesian-penalized likelihood reconstruction for [^{15}O]H_2O myocardial perfusion imaging

Reetta Siekkinen, MSc,[a,b,c] Chunlei Han, PhD,[a] Teemu Maaniitty, MD, PhD,[a] Mika Teräs, PhD,[c,e] Juhani Knuuti, MD, PhD,[a,b] Antti Saraste, MD, PhD,[a,b,d] and Jarmo Teuho, PhD[a,b]

[a] Turku PET Centre, Turku University Hospital, Turku, Finland
[b] Turku PET Centre, University of Turku, Turku, Finland
[c] Department of Medical Physics, Turku University Hospital, Turku, Finland
[d] Heart Centre, Turku University Hospital, Turku, Finland
[e] Institute of Biomedicine, University of Turku, Turku, Finland

Received Feb 22, 2022; accepted Nov 5, 2022
doi:10.1007/s12350-022-03164-5

Background. **New Block-Sequential-Regularized-Expectation-Maximization (BSREM) image reconstruction technique has been introduced for clinical use mainly for oncologic use. Accurate and quantitative image reconstruction is essential in myocardial perfusion imaging with positron emission tomography (PET) as it utilizes absolute quantitation of myocardial blood flow (MBF). The aim of the study was to evaluate BSREM reconstruction for quantitation in patients with suspected coronary artery disease (CAD).**

Methods and Results. **We analyzed cardiac [^{15}O]H_2O PET studies of 177 patients evaluated for CAD. Differences between BSREM and Ordered-Subset-Expectation-Maximization with Time-Of-Flight (TOF) and Point-Spread-Function (PSF) modeling (OSEM-TOF-PSF) in terms of MBF, perfusable tissue fraction, and vascular volume fraction were measured. Classification of ischemia was assessed between the algorithms. OSEM-TOF-PSF and BSREM provided similar global stress MBF in patients with ischemia (1.84 ± 0.21 g·ml^{-1}·min^{-1} vs 1.86 ± 0.21 g·ml^{-1}·min^{-1}) and no ischemia (3.26 ± 0.34 g·ml^{-1}·min^{-1} vs 3.28 ± 0.34 g·ml^{-1}·min^{-1}). Global resting MBF was also similar (0.97 ± 0.12 g·ml^{-1}·min^{-1} and 1.12 ± 0.06 g·ml^{-1}·min^{-1}). The largest mean relative difference in MBF values was 7%. Presence of myocardial ischemia was classified concordantly in 99% of patients using OSEM-TOF-PSF and BSREM reconstructions**

Conclusion. **OSEM-TOF-PSF and BSREM image reconstructions produce similar MBF values and diagnosis of myocardial ischemia in patients undergoing [^{15}O]H_2O PET due to suspected obstructive coronary artery disease (J Nucl Cardiol 2023)**

Key Words: CAD • myocardial ischemia and infarction • PET • MPI • myocardial blood flow • hybrid imaging

Supplementary Information The online version contains supplementary material available at https://doi.org/10.1007/s12350-022-03164-5.

The authors of this article have provided a PowerPoint file, available for download at SpringerLink, which summarises the contents of the paper and is free for re-use at meetings and presentations. Search for the article DOI on SpringerLink.com.

Funding This study has received funding from the Finnish Foundation for Cardiovascular Research (Urho Känkänen Foundation), Paavo Nurmi Foundation, EMPIR programme co-financed by the Participating States and from the European Union's Horizon 2020 research and innovation programme (15HLT05 PerfusImaging, 19SIP04 TracPETperf), from the Academy of Finland (Grant No. 314483, Project MINMOTION), State Research Funding by Turku University Hospital) (Project No. 13236), the Instrumentarium Science Foundation, and Turku University Foundation.

Antti Saraste and Jarmo Teuho have contributed equally to this work.

Reprint requests: Reetta Siekkinen, MSc, Turku PET Centre, Turku University Hospital, Kiinamyllynkatu 4-8, 20520 Turku, Finland; *reetta.siekkinen@tyks.fi*

J Nucl Cardiol
1071-3581/$34.00

Published online: 19 January 2023

Abbreviations	
MPI	Myocardial perfusion imaging
PET	Positron emission tomography
CAD	Coronary artery disease
MBF	Myocardial blood flow
PTF	Perfusable tissue fraction
VL	Vascular volume fraction
BSREM	Block-sequential-regularized-expectation-maximization
OSEM	Ordered-subset-expectation-maximization
TOF	Time-of-flight
PSF	Point-spread-function

INTRODUCTION

Myocardial perfusion imaging (MPI) with Positron emission tomography (PET) can be used as a first line diagnostic test in patients with suspected obstructive coronary artery disease (CAD).[1] MPI PET allows to quantitate myocardial blood flow (MBF), perfusable tissue fraction (PTF), and vascular volume fraction (VL).[2–4] Furthermore, the quantitative MBF during vasodilator stress is a key factor determining myocardial ischemia when compared with intracoronary fractional flow reserve.[5–7] However, such a clinical interpretation can only be made if the PET image reconstruction techniques provide accurate image quantification.[8] Therefore, whenever a new clinical reconstruction technique is introduced, it should be compared against the de facto state-of-the-art reconstruction technique.[9]

Recently, a new reconstruction algorithm Block-Sequential-Regularized-Expectation-Maximization (BSREM, vendor name: Q.Clear) was implemented in clinical use.[10] So far, investigations with BSREM have been mainly conducted with [^{18}F]FDG[11–15] in oncology studies, in which sensitive detection of tumors and their metastases is the main focus. However, there are only a few studies where BSREM is applied in dynamic perfusion studies, in which absolute quantitation and detection of ischemia is the main task. Evaluations have been performed with [^{13}N]NH_3 as part of sarcoidosis diagnostics, with analysis of rest perfusion in 21 patients.[16] Very recently, Nordström et al. thoroughly investigated the effect of various reconstruction parameters with [^{15}O]H_2O, including BSREM.[17] The authors reported no significant change in diagnosis but prompted that the findings to be confirmed with a larger number of patients. As MPI PET is nowadays more increasingly used for detection of myocardial ischemia, the impact of BSREM should be investigated in patients with suspected CAD, both at rest and during stress and using various perfusion tracers and its effect on diagnosis should be confirmed.

Previous studies have indicated that physical test objects (phantoms) are practical when evaluating the accuracy of quantitative values derived from PET images against a ground-truth measurement.[18,19] Our group has recently assessed the accuracy of flow measurements in [^{15}O]H_2O MPI PET, using a dynamic PET phantom.[20] In the study, comparison of an Ordered-Subset-Expectation-Maximization with Time-of-Flight and Point-Spread Function modeling (OSEM-TOF-PSF) algorithm and other reconstruction methods, i.e., the BSREM algorithm, resulted in image-derived flow differing 7% at maximum in comparison to the reference flow.[20]

The goal of the present study was to evaluate the accuracy of BSREM quantification of myocardial perfusion and the impact on the classification of ischemia in a large group of patients with suspected CAD. The BSREM was compared to well-established state-of-the-art reconstruction OSEM-TOF-PSF technique.

MATERIALS AND METHODS

Data of 179 subjects undergone stress or rest-stress [^{15}O]H_2O myocardial perfusion imaging due to suspected obstructive coronary artery disease in Turku PET Centre (Turku, Finland) were analyzed retrospectively. The cohort consisted of 63 females and 116 males ageing (mean ± SD) 66 ± 10 years. Their body mass index was 30 ± 6 kg·m^{-2}. There were 75 current or previous smokers, 35 were diabetics and 98 had hypertension. In 17 patients, rest and stress imaging was performed, and 162 had undergone only stress imaging. The Hospital District of Southwest Finland granted permission for the retrospective study (number T93/2019). Due to the retrospective nature of the study, the collection of informed consents from individual subjects was waived.

All subject data was acquired with a digital Discovery MI PET/CT system (DMI-20, GE Healthcare, Milwaukee, US). The DMI-20 PET detector system consists of four detector rings and one ring comprises 136 detector blocks. Each block employs 3 × 6 array of silicon photomultiplier (SiPM) detectors with a 4 × 9 array of lutetium-yttrium oxyorthosilicate (LYSO) crystals with one crystal element size of 3.95 mm × 5.3 mm × 25 mm. The axial and transaxial FOV sizes of the DMI-20 are 20 cm and 70 cm, respectively. The coincidence timing and energy windows are 4.9 ns and 425-650 keV. The system performance details are described in Hsu et al.[21]

Imaging protocol included a CT acquisition for attenuation correction (CTAC) followed by a dynamic PET study with $[^{15}O]H_2O$. The CTAC acquisition parameters were as follows: tube voltage of 120 kV, tube current of 120 mA and noise index of 30.00. The helical full rotation time was 0.5 seconds, while helical thickness was set at 3.75 mm with pitch of 1.375:1 and speed 55 mm/rotation. The CTAC was reconstructed using full 70 cm field-of-view (FOV).

All 179 subjects had undergone dynamic adenosine stress $[^{15}O]H_2O$ PET. Also, 17 subjects had rest PET prior to stress PET. The PET protocol for both rest and stress imaging was as previously reported.[22,23] After allowing radioactivity from the rest PET imaging injection to decay, adenosine infusion was started 2 minutes before the start of the stress PET acquisition, and was infused 140 μg per kilogram of body weight per minute. Patients were injected with 500 MBq bolus of $[^{15}O]H_2O$ from an automatic dispenser (Hidex Oy, Finland), and PET acquisition was started 25 seconds after the bolus injection. PET acquisition lasted 4 minutes and 40 seconds and the data was thereafter binned into dynamic frame lengths of 14×5 seconds, 3×10 seconds, 3×20 seconds and 4×30 seconds.

Two reconstructions for PET data were applied. The first was the three-dimensional OSEM algorithm with TOF and PSF (OSEM-TOF-PSF) (vendor name: VPFX-S) with 3 iterations and 16 subsets. The reconstructed PET FOV was set to 35 cm, with an image matrix of 192×192 and 5.0 mm post filter. The BSREM reconstructions (vendor name: Q.Clear) were performed with a FOV of 35 cm and matrix size of 192×192. In the Discovery MI PET/CT, the beta value of BSREM is set to a value of 350 by default, which we did not modify for this study. The beta value 350 was selected as recommended by the manufacturer.[24] All PET reconstructions were performed using the clinical software installed on the PET/CT system, with software version of pet_col_bb.31.

Of the 179 subjects undergone only stress imaging, two subjects had to be excluded, one due to a failed injection and the other due to missing frames on the BSREM reconstruction. The final dataset consisted of 177 subjects.

All image analysis with quantification was performed using Carimas 2.10 (Turku PET Centre, Finland) by a single observer (CH) with over 20 years of experience in MPI PET image analysis. For comparison of two reconstruction algorithms OSEM-TOF-PSF and BSREM, myocardial segmentation was performed by using similar volumes of interest (VOI). The delineation and corresponding segmentation of the left ventricle was first performed for the OSEM-TOF-PSF reconstructed images after which the VOIs were copied to BSREM reconstructed images without modification. From each VOI, the time-activity curves (TACs) for the input function and myocardial tissue were extracted.

Kinetic modeling designed for $[^{15}O]H_2O$ tracer was performed based on the image-derived TACs and by using the model presented by Iida H. et al.[2–4] which is implemented in Carimas 2.10. In addition to MBF (in units of $ml \cdot g^{-1} \cdot min^{-1}$), the perfusable tissue fraction (PTF, in units of $ml \cdot ml^{-1}$) and vascular volume fraction (VL in units of $ml \cdot ml^{-1}$) were modelled in order to analyze the effect on other quantitative parameters of kinetic modeling, too. The default parameters used for kinetic modeling were as follows: initial guess for MBF, PTF, and VL was 0.5, for partition coefficient 0.9464 and for beta value 0.93. Fitting of the TACs was performed using uniform weighting. Finally, the MBF values were visually analyzed in standard 17- and 3-segment polar maps, and all parameters were exported to Excel spreadsheets.[25] The 17-segment polar maps represent the standard myocardial segments defined by American Heart Association,[25] and the 3-segment polar map represent the standard myocardial territories of the left anterior descending coronary artery (LAD), the left circumflex coronary artery (LCX) and the right coronary artery (RCA).

The spreadsheets containing MBF, PTF, and VL values from the 17- and 3-segments were imported to MATLAB version 2020a (Mathworks Inc. Natick, US). Classification and analysis of subjects was performed automatically using in-house developed software pipeline in MATLAB 2020a. The analysis pipeline consisted of automatic classification of patients to ischemic and non-ischemic groups, followed by visual and statistical analysis. Myocardial ischemia was defined in the presence of stress MBF < 2.3 $ml \cdot g^{-1} \cdot min^{-1}$ in at least two neighboring segments as previously validated.[5] Segments 2, 3, and 17 were excluded from the analysis due to the presence of the fibrotic area of the basal septum in segments 2 and 3, and potential uncertainties in VOI definition in segment 17. In the 3-vessel analysis, ischemia was defined if average stress MBF was < 2.3 $ml \cdot g^{-1} \cdot min^{-1}$ in one of the vessel territories.

For both reconstructions, we measured mean and standard deviation (SD) values from MBF, PTF, and VL over all segments despite whether the segment was ischemic or non-ischemic. Thereafter, we calculated the mean values of the parameters over the groups of patients classified as ischemic and non-ischemic as well as over the rest patients. The results are presented as mean and SD values for each group, as well as the minimum and maximum value per group. Similarly, we measured the mean relative differences between OSEM-TOF-PSF and BSREM as well as SD of mean relative differences per each patient group. MBF values and the

relative differences of MBF values are visualized in boxplots for the whole cohort. In addition, we represent regression plots and Bland–Altman plots in order to determine the correlation of MBF, PTF, and VL between OSEM-TOF-PSF and BSREM. Also, statistical testing between MBF, PTF, and VL values calculated from OSEM-TOF-PSF and BSREM reconstructed images was performed. A two-tailed *t*-test was applied to indicate if there are significant differences in MBF, PTF and VL with different reconstruction algorithms, using $P < 0.05$ as the significance threshold. Statistical comparison was performed for each segment over all patients. Bonferroni–Holm correction with $\alpha = 0.05$ was applied to account for multiple comparisons.

RESULTS

Table 1 presents the mean, SD and range (from minimum to maximum) values measured from subjects classified as ischemic, non-ischemic as well as from the rest subjects for the 17- and 3-segment polar maps. Also, the mean relative differences and SD of differences measured between OSEM-TOF-PSF and BSREM are presented for each patient group. The measured MBF, PTF and VL values are similar ($P > .5$) between OSEM-TOF-PSF and BSREM. The absolute differences are smaller than 0.5 $ml \cdot g^{-1} \cdot min^{-1}$, 0.1, and 0.1, respectively. The relative mean differences between OSEM-TOF-PSF and BSREM are smaller than 4%, 2%, and 6% for stress studies (non-ischemic and ischemic) and 7%, 4% and 6% for rest studies, for MBF, PTF, and VL in Table 1.

Figure 1 presents the boxplots of relative differences between OSEM-TOF-PSF and BSREM (a, b) and the absolute values (c, d) of segmental MBFs from the 17- (Figure 1a, c) and 3-segment (Figure 1b, c) polar maps for the whole patient cohort. The segmental boxplots show that the median MBF differences are near zero and the quantiles of MBF differences are smaller than 5%. Similarly, the absolute values show no clear difference between the reconstructions for any segment (Figure 1c, d). Also, there is no clear difference between the 3- and 17-segmental boxplots (Figure 1a, b).

Figure 2 shows the correlation analysis for segmental MBF, PTF, and VL obtained using OSEM-TOF-PSF and BSREM reconstructions. The R^2 values of the regression lines were larger than 0.97, 0.97 and 0.98, for stress studies (non-ischemic and ischemic) and 0.98, 0.93, and 1.0 for rest studies, for MBF, PTF, and VL for both 17- and 3-segments. The intercept of the regression line is very close to zero for all parameters and segments (Figure 2).

Figure 3 shows Bland–Altman plots of segmental MBF, PTF, and VL obtained using OSEM-TOF-PSF and BSREM reconstructions. The mean bias between OSEM-TOF-PSF and BSREM is near zero for all parameters and segments. The Lines-of-Agreement (LoAs) are smaller than 0.3 $ml \cdot g^{-1} \cdot min^{-1}$ (Figure 3a), 0.05 (Figure 3b), and 0.04 (Figure 3c) for MBF, PTF, and VL in both 17- and 3-segment plots. Non-ischemic patients show largest variation between OSEM-TOF-PSF and BSREM compared to ischemic and rest subjects.

The 17- and 3 segment MBF polar maps appeared visually similar between OSEM-TOF-PSF and BSREM reconstructions.

OSEM-TOF-PSF classified 115 out of 177 subjects ischemic (MBF < 2.3 $ml \cdot g^{-1} \cdot min^{-1}$ in at least two contiguous segments) from the 17-segment polar maps. The corresponding number was 113 for the BSREM reconstruction. All patients were classified similarly from the 3-segment polar maps with both reconstructions.

Figure 4 presents the 17-segment polar maps of the patients with discrepant classification between OSEM-TOF-PSF (Figure 4a, c) and BSREM (Figure 4b, d) based on the definition by Danad et al.[5] The overall visual impression is similar for both patients. In one patient, OSEM-TOF-PSF classified four segments ischemic, whereas BSREM classified only one segment ischemic. In the other patient, OSEM-TOF-PSF classified five segments ischemic and BSREM two segments. MBF, PTF, and VL values for each segment are presented in Supplementary File I.

DISCUSSION

We performed a retrospective evaluation of the recently introduced BSREM reconstruction algorithm in comparison to the OSEM-TOF-PSF algorithm for the quantitation of myocardial perfusion using $[^{15}O]H_2O$ MPI PET. Data from 177 subjects with suspected obstructive coronary artery disease undergone adenosine stress or rest-stress MPI were evaluated. Both algorithms provided similar absolute values across a wide range of MBF in ischemic myocardial regions and in the normal myocardium. Furthermore, classification of myocardial ischemia was highly concordant with BSREM and OSEM-TOF-PSF.

In general, BSREM showed the largest mean relative differences of 4%, 2%, and 6% for the stress studies and 7%, 4% and 6% for the rest studies in comparison to OSEM-TOF-PSF for MBF, PTF, and VL, respectively (Table 1). These values are similar to our previous study where the flow values differed 7% between the reconstructions on average on a dynamic PET flow phantom.[20] Similarly, the segmental boxplots showed that BSREM produced no more than 5%

Table 1. MBF, PTF, and VL derived by kinetic modeling presented as mean, standard deviation (SD), minimum, and maximum values as well as relative differences between OSEM-TOF-PSF and BSREM at 17 segments and 3 segments

	17 segments		3 segments	
	OSEM Mean ± SD (Min − max) Mean diff (%) ± SD diff (%)	BSREM Mean ± SD (Min − max)	OSEM Mean ± SD (Min − max) Mean diff (%) ± SD diff (%)	BSREM Mean ± SD (Min − max)
	MBF ($ml \cdot g^{-1} \cdot min^{-1}$)			
Ischemic	1.84 ± 0.21 (1.34–2.11) 3.18% ± 2.97%	1.86 ± 0.21 (1.35–2.14)	1.85 ± 0.06 (1.71–2) 2.24% ± 2.03%	1.86 ± 0.07 (1.72–2.04)
Non-ischemic	3.26 ± 0.34 (2.47–3.75) 3.32% ± 2.13%	3.28 ± 0.34 (2.51–3.78)	3.31 ± 0.17 (3.15–3.53) 2.54% ± 2%	3.33 ± 0.17 (3.17–3.56)
Rest	0.97 ± 0.12 (0.77–1.15) 6.59% ± 3.58%	1 ± 0.13 (0.8–1.18)	1.12 ± 0.06 (1.05–1.18) 3.07% ± 2.61%	1.15 ± 0.1 (1.04–1.26)
	PTF			
Ischemic	0.77 ± 0.06 (0.67–0.86) 1.84% ± 1.73%	0.77 ± 0.06 (0.66–0.87)	0.76 ± 0.04 (0.72–0.8) 1.31% ± 1.15%	0.77 ± 0.04 (0.72–0.81)
Non-ischemic	0.76 ± 0.06 (0.65–0.87) 2.13% ± 1.83%	0.77 ± 0.07 (0.65–0.88)	0.76 ± 0.04 (0.71–0.81) 1.76% ± 1.38%	0.77 ± 0.04 (0.71–0.81)
Rest	0.72 ± 0.04 (0.65–0.78) 3.58% ± 6.44%	0.71 ± 0.04 (0.65–0.77)	0.72 ± 0.02 (0.7–0.74) 2.07% ± 2.72%	0.72 ± 0.02 (0.7–0.74)
	VL			
Ischemic	0.22 ± 0.06 (0.13–0.36) 5.49% ± 4.99%	0.21 ± 0.06 (0.13–0.35)	0.21 ± 0.04 (0.17–0.27) 3.8% ± 3.22%	0.21 ± 0.04 (0.16–0.26)
Non-ischemic	0.24 ± 0.06 (0.14–0.37) 5.86% ± 5.86%	0.24 ± 0.06 (0.14–0.36)	0.23 ± 0.04 (0.23–0.29) 3.79% ± 3.09%	0.23 ± 0.04 (0.19–0.28)
Rest	0.22 ± 0.06 (0.15–0.34) 5.15% ± 5.17%	0.22 ± 0.05 (0.14–0.34)	0.22 ± 0.03 (0.19–0.25) 3.66% ± 2.49%	0.22 ± 0.03 (0.18–0.25)

There were no significant differences in any parameters between the reconstruction methods ($P > .05$)

(Figure 1a, b) difference to OSEM-TOF-PSF in terms of medians and quantiles, and no clear differences were noted in terms of absolute values (Figure 1c, d) in whole patient cohort. Furthermore, the R^2 values from the correlation analysis were larger than 0.93 for all parameters and segments in the whole study population (Figure 2). What is more, patients classified non-ischemic showed larger variation between OSEM-TOF-PSF and BSREM reconstructions in Bland–Altman plots (Figure 3) compared to ischemic and rest subjects. However, we consider this variation negligible since the

bias was very close to zero and the LoAs were smaller than 0.5 for all parameters across the group.

The BSREM-based classification was concordant to OSEM-TOF-PSF in 99% (175 out of 177) of subjects based on the threshold of ischemia that has been previously defined in Danad et al.[5] BSREM classified the subjects ischemic and OSEM-TOF-PSF non-ischemic. However, the visual interpretation from the BSREM polar maps indicated only very small differences to OSEM-TOF-PSF for these subjects (Figure 4) caused by random noise and MBF variability close to threshold of ischemia.[5] Ultimately, the time-activity-curves (TACs) (not shown here) were also similar for these subjects between OSEM-TOF-PSF and BSREM. The differences in the PTF and VL parameters between OSEM-TOF-PSF and BSREM were also small. The PTF parameter is defined as the fraction of tissue capable of rapidly exchanging $[^{15}O]H_2O$ within a given volume of region of interest. Therefore, it plays a role in the differentiation of viable myocardium from infarct scar.[26] Our study shows similar PTF values using either OSEM-TOF-PSF or BSREM reconstruction suggesting feasibility in assessment of myocardial viability. The VL parameter is not currently used in clinical interpretation but our study indicates it to remain similar between OSEM-TOF-PSF and BSREM.

BSREM reconstruction has been previously studied widely in the field of oncology with $[^{18}F]$FDG, where superior standardized-uptake-values (SUVs) compared to OSEM-TOF-PSF have been demonstrated.[11–15] Previously, O'Doherty et al. evaluated the MBF values in BSREM reconstruction in rest $[^{13}N]NH_3$ MPI for 21

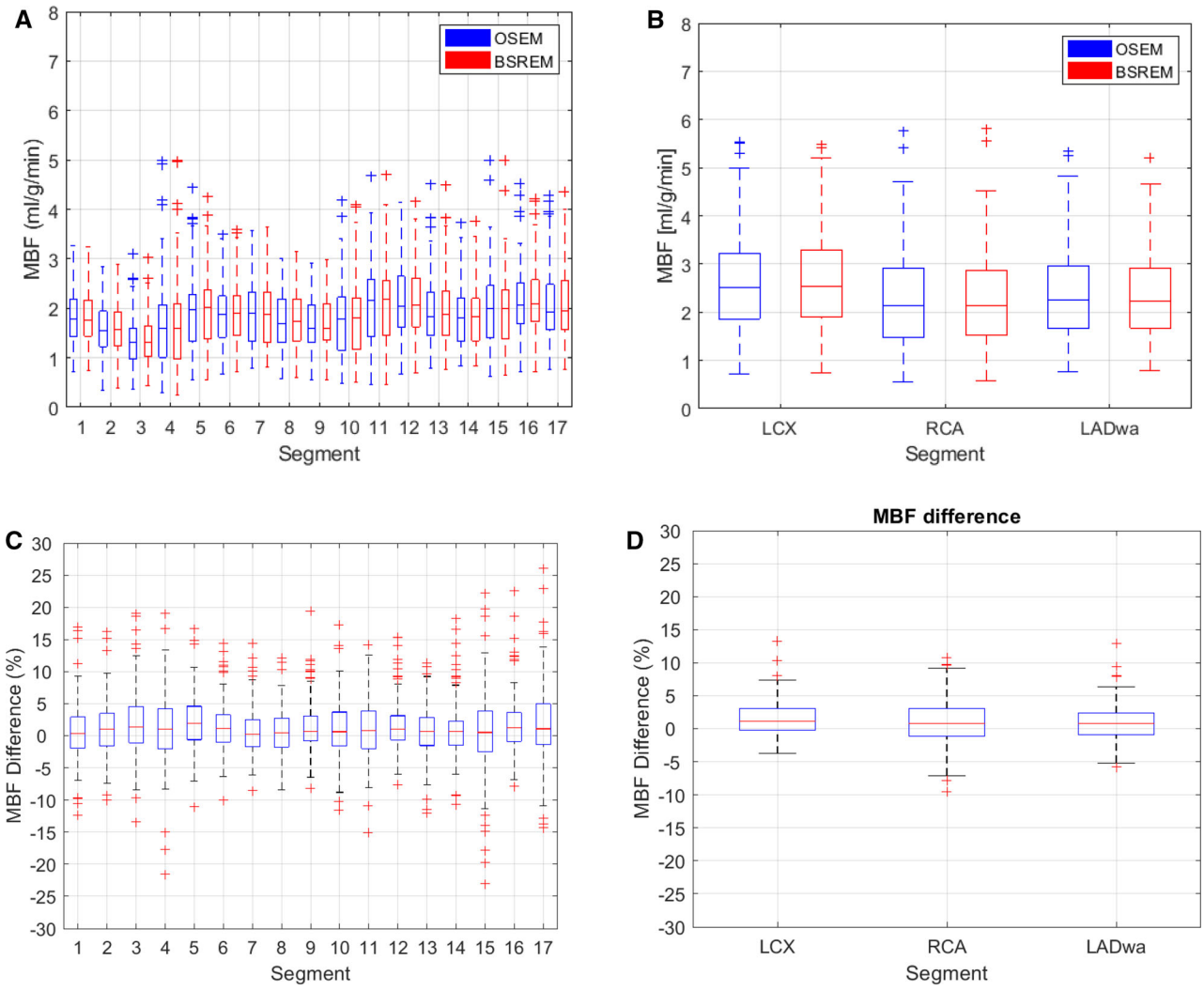

Figure 1. Boxplots of relative differences (**a**, **b**) and absolute values (**c**, **d**) of segmental MBF in whole patient group between OSEM-TOF-PSF and BSREM presented for the **a**, **c**) 17- and **b**, **d**) 3-segment polar maps.

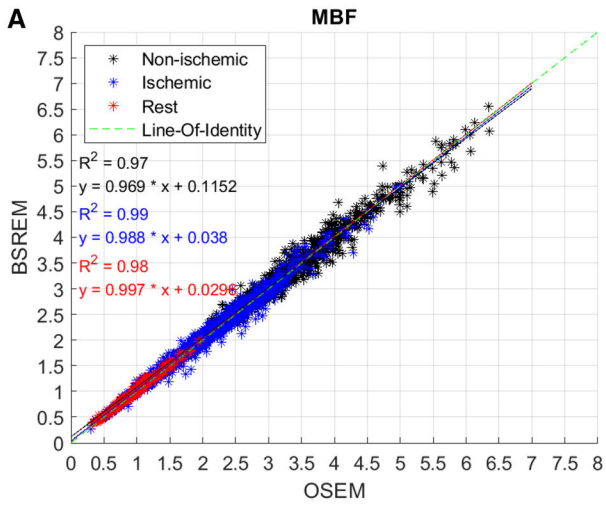
A
MBF
Non-ischemic
Ischemic
Rest
Line-Of-Identity
R2 = 0.97
y = 0.969 * x + 0.1152
R2 = 0.99
y = 0.988 * x + 0.038
R2 = 0.98
y = 0.997 * x + 0.0296
BSREM
OSEM

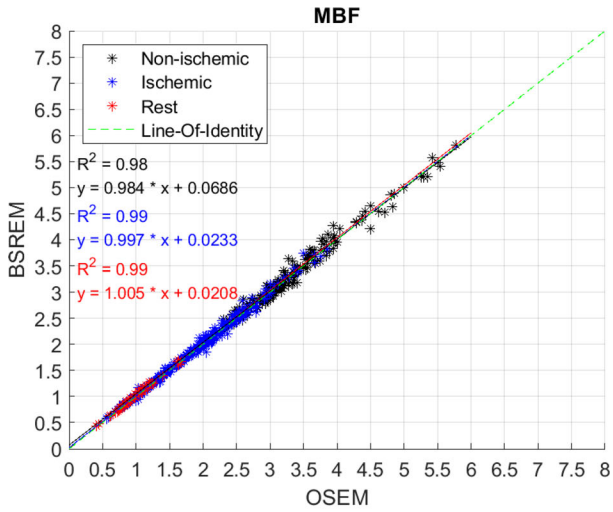
MBF
Non-ischemic
Ischemic
Rest
Line-Of-Identity
R2 = 0.98
y = 0.984 * x + 0.0686
R2 = 0.99
y = 0.997 * x + 0.0233
R2 = 0.99
y = 1.005 * x + 0.0208
BSREM
OSEM

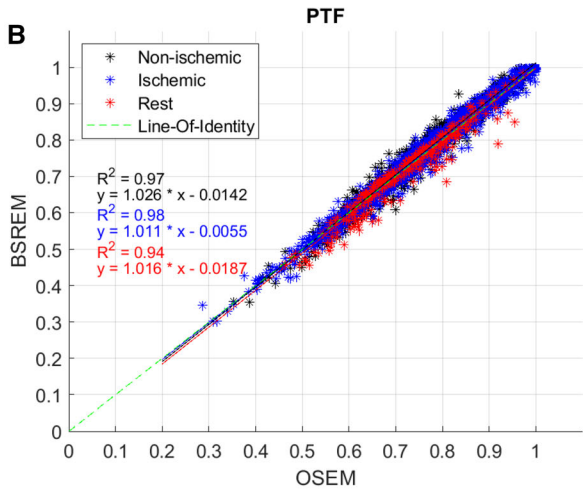
B
PTF
Non-ischemic
Ischemic
Rest
Line-Of-Identity
R2 = 0.97
y = 1.026 * x - 0.0142
R2 = 0.98
y = 1.011 * x - 0.0055
R2 = 0.94
y = 1.016 * x - 0.0187
BSREM
OSEM

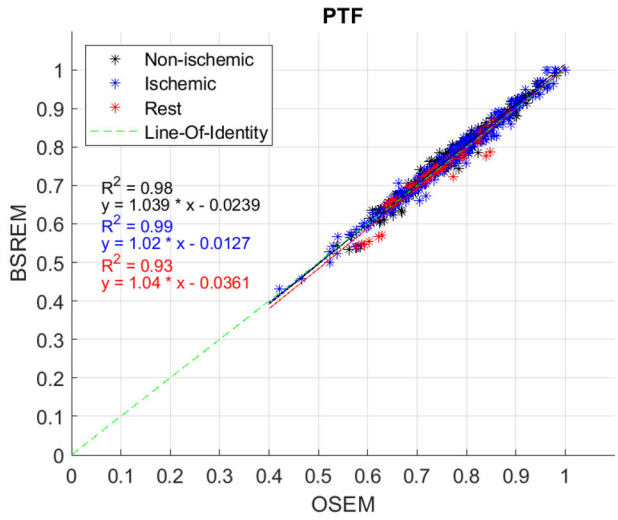
PTF
Non-ischemic
Ischemic
Rest
Line-Of-Identity
R2 = 0.98
y = 1.039 * x - 0.0239
R2 = 0.99
y = 1.02 * x - 0.0127
R2 = 0.93
y = 1.04 * x - 0.0361
BSREM
OSEM

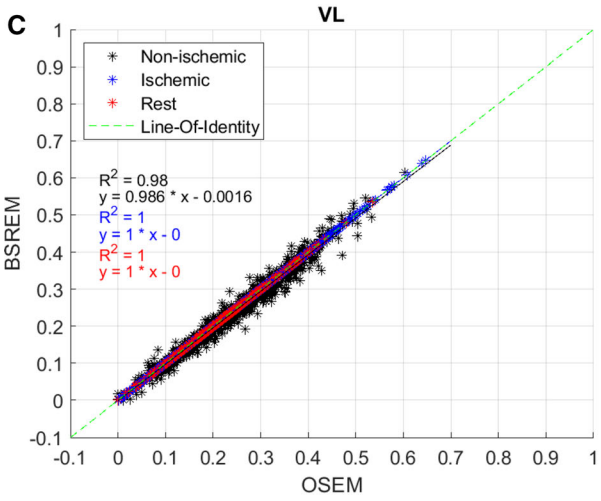
C
VL
Non-ischemic
Ischemic
Rest
Line-Of-Identity
R2 = 0.98
y = 0.986 * x - 0.0016
R2 = 1
y = 1 * x - 0
R2 = 1
y = 1 * x - 0
BSREM
OSEM

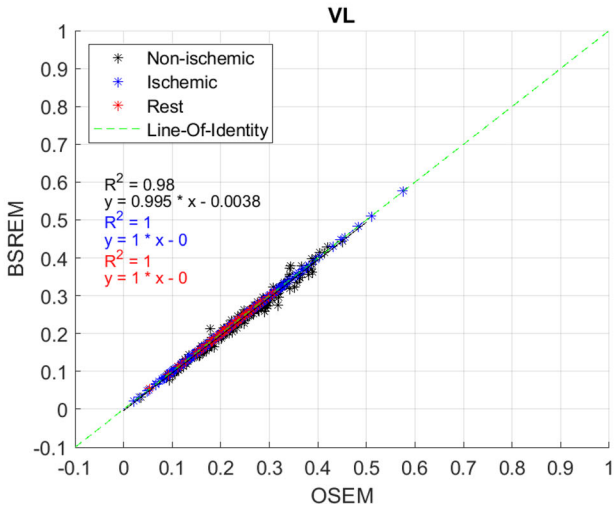
VL
Non-ischemic
Ischemic
Rest
Line-Of-Identity
R2 = 0.98
y = 0.995 * x - 0.0038
R2 = 1
y = 1 * x - 0
R2 = 1
y = 1 * x - 0
BSREM
OSEM

◀**Figure 2.** Correlation analysis of segmental **a** MBF ($ml \cdot g^{-1} \cdot min^{-1}$), **b** PTF and **c** VL obtained using OSEM-TOF-PSF and BSREM reconstructions. Segments of non-ischemic (black) and ischemic (blue) patients as well as rest (red) studies are shown in different colors. The line-of-identity is visualized in green. Results for 17 segments are shown in the left column and 3 segments (LAD, RCA, and LCX) in the right column.

subjects.[16] The study showed that the resting MBF values are closely correlated ($P > .95$) across BSREM and other reconstructions.[16] Similarly, Nordström et al. found only minor differences in MBF quantification between various reconstructions for [^{15}O]H_2O.[17] The findings of our study complement these results, as no significant difference was measured between OSEM-TOF-PSF and BSREM ($P > .05$) in patients with suspected CAD studied at rest and during stress using a large patient group. However, no such studies have been performed for [^{82}Rb], to the best knowledge of the authors.

In addition to reconstruction algorithms, other factors contribute to variability in quantification of MBF. El Fakhri et al. have studied the reproducibility of MBF quantitation with [^{82}Rb] and [^{13}N]-NH_3.[27] They reported test–retest repeatability of 16% for stress MBF. Similar test–retest repeatability has been observed with [^{15}O]H_2O PET.[28] Nesterov et al. have studied intra- and inter-observer repeatability of MBF quantification with the Carimas software used in this study.[29] They reported intra-observer difference of 9% and inter-observer difference of 10% for analysis of MBF.[29] Moreover, Nordström et al. reported an intra-and inter-observer variability of less than few percent, which can be considered to be within the limits of the inherent uncertainty of MBF measurements in their study.[30] As our largest difference for any parameter was 7% we consider that these results fall below the day-to-day and intra- and inter-observer uncertainty.

We have also shown that there is only a minor difference in measured MBF between BSREM and OSEM-TOF-PSF, similarly to very recent study of Nordström et al.[17] This may be partly explained by [^{15}O]H_2O relying on wash out/k2-based flow estimates in contrast to other perfusion tracers relying on wash in/K1-based flow estimates, which also stabilizes MBF quantification across various reconstruction options such as changing the beta value.[17] For PTF, an effect might be observed if the tissue fraction within a delineated VOI would change drastically between reconstructions. However, this would need to be systematically studied in detail. The results of the study of Nordström et al.[17] would indicate that the effect of different reconstructions as well as different beta values to PTF are minimal.

Moreover, non-TOF and non-PSF algorithms were not compared in this study as we applied two state-of-the-art reconstructions available on a clinical PET/CT system. Previous studies performed by Armstrong et al.[31] and Germino et al.[32] have shown that incorporation of TOF and PSF is beneficial for MBF quantification. Armstrong et al. showed improvement in accuracy of MBF values when applying OSEM-TOF-PSF in 37 patients undergone [^{82}Rb] PET perfusion imaging.[31] In addition, Germino et al. showed that OSEM-TOF-PSF reconstruction reduces standard error of estimated kinetic parameters and improves quality of parametric [^{82}Rb] and [^{15}O]H_2O images.[32]

In our study, small differences in MBF between OSEM-TOF-PSF and BSREM can be partly explained by incorporation of both TOF and PSF modeling in both OSEM-TOF-PSF and BSREM reconstructions. Image quality was also similar between the two algorithms, in line with O'Doherty et al. who reported similar [^{13}N]NH_3 image noise between OSEM-TOF and BSREM when beta values of 300 to 400 are used.

As a limitation to this study, only one analysis software (Carimas) with specific modeling for [^{15}O]H_2O[2–4] was used. However, good comparability and reproducibility has been shown across various software for MBF analysis.[29] Our results also complement the assumption of Norström et al.[17] who applied a different analysis software for [^{15}O]H_2O, indicating that [^{15}O]H_2O quantification should be robust across various software.

Previous studies have also experimented several beta values (for example 100-1000 in Teoh et al.[15]) in BSREM reconstruction and their impact on the image quality. However, we applied only one beta value (350) due to the retrospective nature of our study. The beta value used in this study is routinely applied in MPI studies at our institute and is the default value set in the Discovery MI 20 4-ring system. This is close to the value of 400 recommended by Teoh et al.[15] and value of 300 to 400 recommended by O'Doherty et al.[16] Thus, the results of this study could be applied immediately in the clinical routine by using the default beta value (350) for the DMI system recommended by the manufacturer, enabling the use of BSREM for MBF quantification in [^{15}O]H_2O MPI PET.

NEW KNOWLEDGE GAINED

Myocardial perfusion imaging using [^{15}O]H_2O PET can be conducted applying either OSEM-TOF-PSF or BSREM (using a beta value of 350) reconstructions without any significant differences in terms of MBF, PTF and VL. The relative differences between OSEM-TOF-PSF and BSREM are smaller than 7%. Both

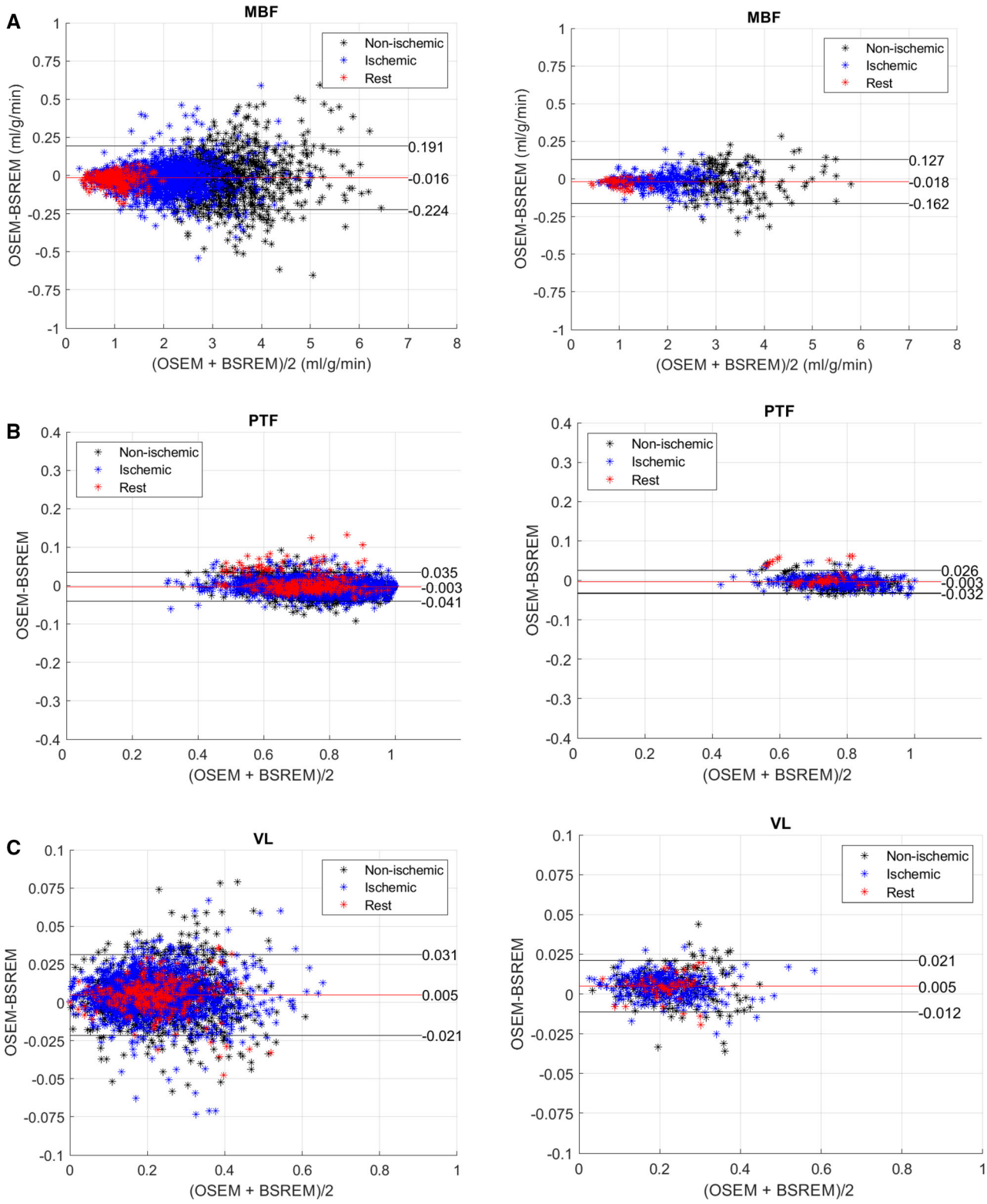

Figure 3. Bland–Altman scatter plots of segmental **a** MBF ($ml \cdot g^{-1} \cdot min^{-1}$), **b** PTF, and **c** VL obtained using BSREM and OSEM-TOF-PSF reconstructions. Results for 17 segments are shown in the left column and 3 segments (LAD, RCA and LCX) in the right column.

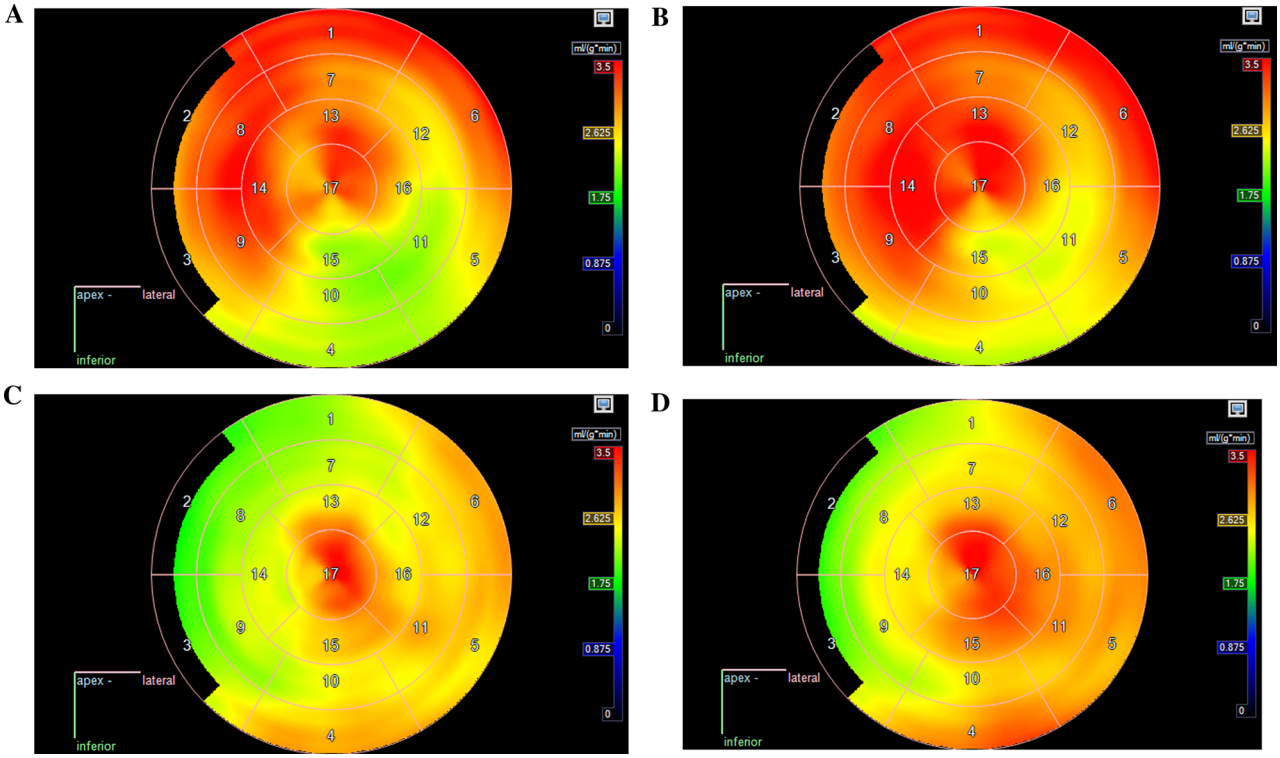

Figure 4. The 17-segment polar maps of the two subjects classified discordantly between OSEM-TOF-PSF and BSREM based on the definition by Danad et al.[5] In **a** OSEM-TOF-PSF (1st patient) and **b** BSREM (1st patient), **c** OSEM-TOF-PSF (2nd patient) and **d** BSREM (2nd patient) reconstructions are presented. The patients were classified ischemic based on the OSEM-TOF-PSF reconstruction and non-ischemic based on the BSREM reconstruction.

reconstructions produce similar classification of ischemia.

CONCLUSIONS

BSREM with beta value of 350 and OSEM-TOF-PSF algorithms provide similar quantification of MBF, PTF, and VL and result to similar classification of ischemia using $[^{15}O]H_2O$ MPI PET in patients with suspected CAD.

Acknowledgements

This study was conducted within the Finnish Center of Excellence in Molecular Imaging in Cardiovascular and Metabolic Research supported by the Academy of Finland, University of Turku, Turku University Hospital and Åbo Akademi University.

Funding

Open Access funding provided by University of Turku (UTU) including Turku University Central Hospital.

Disclosures

The authors declare no conflict of interest.

References

1. Neumann FJ, Sechtem U, Banning AP, et al. 2019 ESC Guidelines for the diagnosis and management of chronic coronary syndromes. Eur Heart J 2020;41:407-77.
2. Iida H, Kanno I, Takahashi A, et al. Measurement of absolute myocardial blood flow with H2150 and dynamic positron emission tomography: Strategy for quantification in relation to the partial volume effect. Circulation 1988;78:104-15. https://doi.org/10.1161/01.CIR.78.1.104.
3. Iida H, Rhodes CG, Desilva R, et al. Myocardial tissue fraction: Correction for partial volume effects and measure of tissue viability. J Nucl Med 1991;32:2169-75.
4. Iida H, Rhodes CG, de Silva R, et al. Use of the left ventricular time-activity curve as a noninvasive input function in dynamic

oxygen-15-water positron emission tomography. J Nucl Med 1992;33:1669-77.
5. Danad I, Uusitalo V, Kero T, et al. Quantitative assessment of myocardial perfusion in the detection of significant coronary artery disease: Cutoff values and diagnostic accuracy of quantitative [15O]H2O PET imaging. J Am Coll Cardiol 2014;64:1464-75. https://doi.org/10.1016/j.jacc.2014.05.069.
6. Knuuti J, Ballo H, Juarez-Orozco LE, et al. The performance of non-invasive tests to rule-in and rule-out significant coronary artery stenosis in patients with stable angina: A meta-analysis focused on post-test disease probability. Eur Heart J 2018;39:3322-30. https://doi.org/10.1093/eurheartj/ehy267.
7. Sciagrà R, Lubberink M, Hyafil F, et al. EANM procedural guidelines for PET/CT quantitative myocardial perfusion imaging. Eur J Nucl Med Mol Imaging 2021;48:1040-69. https://doi.org/10.1007/s00259-020-05046-9.
8. Moody JB, Lee BC, Corbett JR, et al. Precision and accuracy of clinical quantification of myocardial blood flow by dynamic PET: A technical perspective. J Nucl Cardiol 2015;22:935-51. https://doi.org/10.1007/s12350-015-0100-0.
9. Aide N, Lasnon C, Desmonts C, et al. Advances in PET-CT technology: An update. Semin Nucl Med 2021. https://doi.org/10.1053/j.semnuclmed.2021.10.005.
10. Ross S (2014) Q.Clear. GE Healthc
11. te Riet J, Rijnsdorp S, Roef MJ, Arends AJ. Evaluation of a Bayesian penalized likelihood reconstruction algorithm for low-count clinical 18F-FDG PET/CT. EJNMMI Phys 2019. https://doi.org/10.1186/s40658-019-0262-y.
12. Dolci C, Spadavecchia C, Crivellaro C, et al. Treatment response assessment in [18 F]FDG-PET/CT oncology scans: Impact of count statistics variation and reconstruction protocol. Phys Medica 2019;57:177-82. https://doi.org/10.1016/j.ejmp.2018.12.038.
13. Matti A, Lima GM, Pettinato C, et al. How do the more recent reconstruction algorithms affect the interpretation criteria of PET/CT images? Nucl Med Mol Imaging 2019;53:216-22. https://doi.org/10.1007/s13139-019-00594-x.
14. Messerli M, Stolzmann P, Egger-Sigg M, et al. Impact of a Bayesian penalized likelihood reconstruction algorithm on image quality in novel digital PET/CT: Clinical implications for the assessment of lung tumors. EJNMMI Phys 2018. https://doi.org/10.1186/s40658-018-0223-x.
15. Teoh EJ, McGowan DR, Macpherson RE, et al. Phantom and clinical evaluation of the Bayesian penalized likelihood reconstruction algorithm Q.Clear on an LYSO PET/CT system. J Nucl Med 2015;56:1447-52. https://doi.org/10.2967/jnumed.115.159301.
16. O'Doherty J, McGowan DR, Abreu C, Barrington S. Effect of Bayesian-penalized likelihood reconstruction on [13N]-NH3 rest perfusion quantification. J Nucl Cardiol 2017;24:282-90. https://doi.org/10.1007/s12350-016-0554-8.
17. Norström J, Lindström E, Kero T, et al. Influence of image reconstruction on quantitative cardiac 15O-water positron emission tomography. J Nucl Cardiol 2022. https://doi.org/10.1007/s12350-022-03075-5.
18. Gabrani-Juma H, Clarkin OJ, Pourmoghaddas A, et al. Validation of a multimodality flow phantom and its application for assessment of dynamic SPECT and PET technologies. IEEE Trans Med Imaging 2016;36:132-41.
19. Doherty J, Chalampalakis Z, Schleyer P, et al. The effect of high count rates on cardiac perfusion quantification in a simultaneous PET-MR system using a cardiac perfusion phantom. EJNMMI Phys 2017. https://doi.org/10.1186/s40658-017-0199-y.
20. Siekkinen R, Teuho J, Smith NAS, et al. Study of the effect of reconstruction parameters for myocardial perfusion imaging in PET with a novel flow phantom. Front Phys 2020;8:1-10. https://doi.org/10.3389/fphy.2020.00148.
21. Hsu DFC, Ilan E, Peterson WT, et al. Studies of a next-generation silicon-photomultiplier–based time-of-flight PET/CT system. J Nucl Med 2017;58:1511-8. https://doi.org/10.2967/jnumed.117.189514.
22. Kajander S, Joutsiniemi E, Saraste M, et al. Cardiac positron emission tomography/computed tomography imaging accurately detects anatomically and functionally significant coronary artery disease. Circulation 2010;122:603-13. https://doi.org/10.1161/CIRCULATIONAHA.109.915009.
23. Stenström I, Maaniitty T, Uusitalo V, et al. Frequency and angiographic characteristics of coronary microvascular dysfunction in stable angina: A hybrid imaging study. Eur Heart J Cardiovasc Imaging 2017;18:1206-13. https://doi.org/10.1093/ehjci/jex193.
24. Chicheportiche A, Marciano R, Orevi M. Comparison of NEMA characterizations for Discovery MI and Discovery MI-DR TOF PET/CT systems at different sites and with other commercial PET/CT systems. EJNMMI Phys 2020. https://doi.org/10.1186/s40658-020-0271-x.
25. Bom MJ, Schumacher SP, Driessen RS, et al. Impact of individualized segmentation on diagnostic performance of quantitative positron emission tomography for haemodynamically significant coronary artery disease. Eur Heart J Cardiovasc Imaging 2019;20:525-32. https://doi.org/10.1093/ehjci/jey201.
26. Grönman M, Tarkia M, Stark C, et al. Assessment of myocardial viability with [15O]water PET: A validation study in experimental myocardial infarction. J Nucl Cardiol 2021;28:1271-80. https://doi.org/10.1007/s12350-019-01818-5.
27. El Fakhri G, Kardan A, Sitek A, et al. Reproducibility and accuracy of quantitative myocardial blood flow assessment with 82Rb PET: Comparison with 13N-ammonia PET. J Nucl Med 2009;50:1062-71. https://doi.org/10.2967/jnumed.104.007831.
28. Johansson BL, Sundell J, Ekberg K, et al. C-peptide improves adenosine-induced myocardial vasodilation in type 1 diabetes patients. Am J Physiol 2004;286:14-9. https://doi.org/10.1152/ajpendo.00236.2003.
29. Nesterov SV, Han C, Mäki M, et al. Myocardial perfusion quantitation with 15O-labelled water PET: High reproducibility of the new cardiac analysis software (Carimas™). Eur J Nucl Med Mol Imaging 2009;36:1594-602. https://doi.org/10.1007/s00259-009-1143-8.
30. Nordström J, Harms HJ, Kero T, et al. Effect of PET-CT misalignment on the quantitative accuracy of cardiac 15O-water PET. J Nucl Cardiol 2022;29:1119-28. https://doi.org/10.1007/s12350-020-02408-6.
31. Armstrong IS, Tonge CM, Arumugam P. Impact of point spread function modeling and time-of-flight on myocardial blood flow and myocardial flow reserve measurements for rubidium-82 cardiac PET. J Nucl Cardiol 2014;21:467-74. https://doi.org/10.1007/s12350-014-9858-8.
32. Germino M, Ropchan J, Mulnix T, et al. Quantification of myocardial blood flow with 82Rb: Validation with 15O-water using time-of-flight and point-spread-function modeling. EJNMMI Res 2016. https://doi.org/10.1186/s13550-016-0215-6.